

Mini Review

## Structure-Chemical Analysis of Multiple Complexations by Cyclodextrins

NORIAKI FUNASAKI

Kyoto Pharmaceutical University, Misasagi, Yamashina-ku, Kyoto 607-8414, Japan; e-mail: funasaki@mb.kyoto-phu.ac.jp

(Received: 19 September 2003; in final form: 9 October 2003)

**Key words:** bivalent substrates, cyclodextrins, multiple equilibria, NMR chemical shift, solution structure

### Abstract

The interactions between cyclodextrin and substrates having two binding sites in aqueous solution are reviewed. For such substrates, multiple equilibria, NMR chemical shift variations with full binding, solution structures of complexes, and the effect of cavity size are analyzed quantitatively. After general treatments of multiple equilibria and chemical shifts are given, they are applied to three bivalent substrates of diheptanoyllecithin, dialkyldimethylammonium bromide, and oxyphenonium bromide for demonstrating their usefulness. The solution structures of complexes play a crucial role in these basic researches as well as the applications of cyclodextrins, such as bitter taste reduction and stabilization of labile substrates.

**Abbreviations:** CD = D – Cyclodextrin; DDAB – didecyldimethylammonium bromide; DHPC – diheptanoyllecithin; G<sup>+</sup> – gauche<sup>+</sup>; G<sup>-</sup> – gauche<sup>-</sup>; HDOAB – hexyldimethyloctylammonium bromide; OB – oxyphenonium bromide; ROESY – rotating frame Overhauser enhancement spectroscopy; S – substrate; SD – standard deviation; T – trans; XY – bivalent substrate.

### Introduction

Cyclodextrins (CDs) are doughnut-shaped molecules, formed from D(+)-glucose units linked in a cycle. The interior of the doughnut predominantly contains CH groups and it provides, therefore, a relatively hydrophobic environment into which nonpolar molecules can be trapped [1, 2]. The stoichiometry, binding constants, structures, and chemical reactivity of CD complexes have been summarized in books and reviews [1–11].

The cavity of cyclohexaamylose ( $\alpha$ CD) has a diameter of approximately 0.45 nm. This  $\alpha$ CD cavity, therefore, can accommodate surfactants very well. Cyclooctaamylose ( $\gamma$ CD) has a large cavity enough to accommodate two alkyl chains simultaneously and cycloheptaamylose ( $\beta$ CD) has an intermediate cavity between  $\alpha$ CD and  $\gamma$ CD. Bivalent substrates that have two binding sites to CDs can form more complexes with CDs than univalent substrates. In this review, the binding constants and solution structures of CD complexes with bivalent substrates will be surveyed in special emphasis with the quantitative relationship between the solution structure and the binding constant.

### Multiple equilibria

From the macroscopic viewpoint a bivalent substrate (S) forms the 1:1 (SD) and 1:2 (SD<sub>2</sub>) complexes with two CD (D) molecules stepwise [8, 11]:



The macroscopic 1:1 binding constant  $K_1$  and 1:2 binding constant  $K_2$  are defined as

$$K_1 = [SD]/[S][D] \quad (1)$$

$$K_2 = [SD_2]/[SD][D] \quad (2)$$

From the microscopic viewpoint the bivalent substrate (XY) has two binding sites, X and Y. It can form two 1:1 complexes, XDY (X-in complex) and XYD (Y-in complex) simultaneously and these 1:1 complexes can form a 1:2 complex (XDYD) stepwise. Then, we can define two microscopic 1:1 binding constants ( $k_{1X}$  and  $k_{1Y}$ ) and two microscopic 1:2 binding constants ( $k_{2Y}$  and  $k_{2X}$ ) as:

$$k_{1X} = [XDY]/[XY][D] \quad (3)$$

$$k_{1Y} = [XYD]/[XY][D] \quad (4)$$

$$k_{2Y} = [XDYD]/[XDY][D] \quad (5)$$

$$k_{2X} = [XDYD]/[XYD][D] \quad (6)$$

Because  $[SD] = [XDY] + [XYD]$  and  $[SD_2] = [XDYD]$ , we can obtain the relationships between the macroscopic and microscopic binding constants:

$$K_1 = k_{1X} + k_{1Y} \quad (7)$$

$$K_2 = k_{2Y}k_{2X}/(k_{2Y} + k_{2X}) \quad (8)$$

These Equations (1)–(8) also hold true for acid dissociation of  $\text{NH}_3^+\text{CH}_2\text{COOH}$  (dibasic acid), where the proton takes the role of D. More general treatments for multiple equilibria, such as acid dissociation of polyacids and protein binding, have been given in books and the literature [8, 11–13].

Macroscopic binding constants can be determined by many methods, whereas microscopic constants may be estimated by a limited number of spectroscopic methods, such as NMR, optical absorption, ESR, and fluorescence [11]. Proton chemical shifts have been employed to estimate microscopic binding constants. Microscopic binding constants of a bivalent substrate may be estimated from those of two univalent substrates having the same binding sites as the bivalent substrate [8, 10, 14–16].

Didecyldimethylammonium bromide (DDAB) is an equivalent bivalent substrate where  $X = Y = \text{decyl chain}$ . Oxyphenonium bromide (OB) is a nonequivalent bivalent substrate where  $X$  (phenyl group)  $\neq Y$  (cyclohexyl group). For the equivalent substrate, Equation (7) is reduced to

$$K_1 = 2k_1 \quad (9)$$

when  $k_1 = k_2$ , (the equivalent independent binding), Equation (8) is simplified to

$$K_2 = K_1/4 \quad (10)$$

When  $k_1 \neq k_2$  (the equivalent dependent binding), Equation (10) does not hold. When  $K_2 > K_1/4$ , it is called cooperative binding. When  $K_2 < K_1/4$ , it may be called inhibitory binding. According to Connors, these dependent binding modes are caused by three effects; the electronic effect of S bound at site Y on the nature of site X, the repositioning effect, and the CD–CD interaction effect [8]. These effects will induce some changes in the solution structure of complexes.

### Chemical shift variation

NMR will be the most powerful method for investigation of the structures and properties of solutions. The chemical shift is usually referred to an external or internal standard. The chemical shift referred to the external standard must be corrected to the change in volume magnetic susceptibility with increasing concentration of a substrate or CD, although the standard does not interact with the sample solution. The internal standard method is recommended, if an inert standard is available for the sample solution. The widely used internal standard for NMR studies in aqueous solution

is sodium 4,4-dimethyl-4-silapentane-1-sulfonate. However, because it can interact with CDs, it is not suitable for such studies. For cationic or neutral solutes tetramethylammonium chloride is the best internal standard [17–19]. For anionic and neutral solutes sodium methyl sulfate is a good internal standard [18, 20]. Methanol and water are good internal standards for all solutes in aqueous solution [17–21].

The chemical shift is usually different in the free and bound states. This variation  $\Delta\delta$  ( $\delta_{\text{complex}} - \delta_{\text{free}}$ ) is used to determine the binding constant and the solution structure of a complex. Generally, the chemical shift of a proton near the binding site exhibits a large variation. The solution structures of CD complexes with aromatic substrates were estimated from the chemical shift variation induced by the ring current of the phenyl group [3, 21, 22]. However, the chemical shift variations for an aliphatic substrate are not used to estimate a detailed structure of the complex [3]. Very recently, it has been demonstrated that the chemical shift variation of an aliphatic substrate is closely related with the geometric position in the structure of the complex [23]. This relation may be used to estimate the solution structures of complexes.

When complex formation between S and D is rapid on the NMR time scale, the chemical shift of a substrate proton can be written as

$$\delta = ([S]\delta_S + [SD]\delta_{SD} + [SD_2]\delta_{SD_2})/C_S \quad (11)$$

Here  $\delta_S$ ,  $\delta_{SD}$ , and  $\delta_{SD_2}$  denote the chemical shifts of S, SD, and  $SD_2$ , respectively, and  $C_S$  is the total concentration of substrate. The chemical shift of an  $\alpha$ CD proton can be written as

$$\delta = ([D]\delta_D + [SD]\delta_{SD} + 2[SD_2]\delta_{SD_2})/C_D \quad (12)$$

Here  $\delta_D$  denotes the chemical shifts of the CD proton and  $C_D$  is the total concentration of CD. The macroscopic chemical shift variation with the 1:1 complexation is connected with the microscopic chemical shift variations [14, 22, N. Funasaki *et al.*, submitted for publication]:

$$\begin{aligned} \Delta\delta_{SD} &= (k_{1X}\Delta\delta_{XDY} + k_{1Y}\Delta\delta_{XYD})/K_1 \\ &= x_X\Delta\delta_{XDY} + x_Y\Delta\delta_{XYD} \end{aligned} \quad (13)$$

Here  $\Delta\delta_{XDY}$  and  $\Delta\delta_{XYD}$  stand for the microscopic chemical shift variations with the X-in and Y-in complexes at full binding, respectively. These microscopic variations cannot be determined by experiment, although the macroscopic variation  $\Delta\delta_{SD}$  is obtainable by experiment. The mole fraction  $x_X$  of the X-in complex in the 1:1 complex is equal to  $k_{1X}/K_1$  and that  $x_Y$  of the Y-in complex is  $k_{1Y}/K_1$ . The microscopic chemical shift variations may be used to estimate the mole fraction  $x_X$  or  $x_Y$  [22, N. Funasaki *et al.*, submitted for publication].

## DHPC-CD system

Diheptanoyllecithin (DHPC, Figure 1) has two heptanoyl groups that can bind to CDs. These groups are nonequivalent to each other. The  $\alpha$ -methylene protons of chains 1 and 2 have different chemical shifts. The  $\omega$ -methyl protons of chains 1 and 2 become nonequivalent on  $\alpha$ -CD complexation, as is the case in the micellar state. Furthermore, DHPC has three rotamers, different in the dihedral angle around the C1—C2 bond of the glycerol group (Figure 1). The populations of these rotamers (*gauche*<sup>+</sup>, *gauche*<sup>-</sup>, and *trans*) can be determined from the vicinal spin-spin coupling constants,  $J_{AX}$  and  $J_{BX}$ , of the C<sub>2</sub>H<sub>X</sub>—C<sub>1</sub>H<sub>A</sub>H<sub>B</sub> spin system. In water the *gauche*<sup>+</sup> (*G*<sup>+</sup>) and *gauche*<sup>-</sup> (*G*<sup>-</sup>) rotamers are the major components, whereas the *trans* (*T*) form is the minor component: the two heptanoyl chains are mainly in a parallel arrangement. Thus, DHPC can form six 1:1 complexes with CDs [14, 15].

The chemical shift was referred to external sodium 4,4-dimethyl-4-silapentane-1-sulfonate. The concentration of DHPC was kept constant at 1 mmol kg<sup>-1</sup>, while the concentration of CD was varied. This DHPC concentration is below the critical micelle concentration of 1.5 mmol kg<sup>-1</sup>. The chemical shift was corrected for the volume magnetic susceptibility effect.

From the chemical shifts of DHPC protons, the macroscopic 1:1 and 1:2 binding constants ( $K_1$  and  $K_2$ ) and the chemical shift variations ( $\Delta\delta_{SD}$  and  $\Delta\delta_{SD_2}$ ) were determined. Further, the microscopic 1:1 and 1:2 binding constants for  $\alpha$ CD and chemical shift variations were determined from the chemical shifts of the  $\alpha$ -methylene protons of chains 1 and 2. The difference between chains 1 and 2 is very small. Furthermore, from the vicinal coupling constants  $J_{AX}$  and  $J_{BX}$ , the microscopic 1:1 ( $k_{1G^+}$ ,  $k_{1G^-}$ , and  $k_{1T}$ ) and 1:2 ( $k_{2G^+}$ ,  $k_{2G^-}$ , and  $k_{2T}$ ) binding constants were determined. Among the three microscopic 1:1 binding constants, the largest constant is  $k_{1T}$  for  $\alpha$ CD and  $k_{1G^+}$  for  $\beta$ CD and  $\gamma$ CD, respectively.

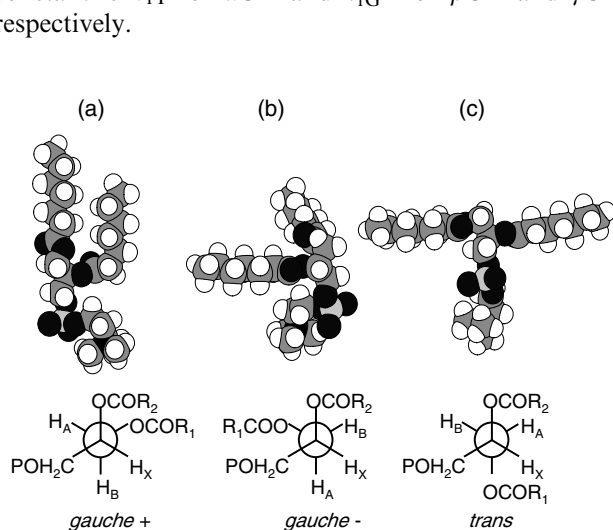


Figure 1. Three rotamers of DHPC: (a) *gauche*<sup>+</sup>, (b) *gauche*<sup>-</sup>, and (c) *trans* [14].

The structures of DHPC complexes with  $\alpha$ CD,  $\beta$ CD, and  $\gamma$ CD were estimated on the basis of the chemical shift variations of DHPC and CD, the vicinal coupling constants of CD, molecular mechanics calculations, and the ROESY spectrum. The structures of three complexes are shown in Figure 2. Regardless of the rotamers of DHPC, one of chains 1 and 2 in the 1:1 complexes will be tightly incorporated in an  $\alpha$ CD cavity (one complex is illustrated in parts a and b). As shown in part c, chains 1 and 2 in the *trans* form of DHPC are separately incorporated in two  $\alpha$ CD molecules. This structure is consistent with the finding that the *trans* form has a larger 1:2 binding constant than the *gauche*<sup>+</sup> and *gauche*<sup>-</sup> forms. As shown in part d, chains 1 and 2 are incorporated in a  $\gamma$ CD cavity simultaneously. This structure is in good agreement with preferential binding of the *gauche*<sup>+</sup> form over the *trans* and *gauche*<sup>-</sup> forms and with nonequivalent signals of the  $\omega$ -methyl protons of chains 1 and 2 induced by complex formation with  $\gamma$ CD [14].

The changes in  $J_{AX}$  and  $J_{BX}$  with addition of  $\beta$ CD are similar to those of  $\gamma$ CD. This finding suggests that the structures of  $\beta$ CD complexes are similar to those of  $\gamma$ CD. The chemical shift variations of CD protons with 1:1  $\beta$ CD complex formation are much larger than those of  $\alpha$ CD and  $\gamma$ CD. Further, six vicinal coupling constants of  $\beta$ CD induced by  $\beta$ CD complex formation are much larger than those by  $\alpha$ CD and  $\gamma$ CD. These findings suggest that the two heptanoyl chains are both incorporated in a  $\beta$ CD cavity and that the macrocycle of  $\beta$ CD is remarkably deformed. Keeping these images in mind, we constructed an initial structure of the 1:1  $\beta$ CD complex and optimized by molecular mechanics calculations. The optimized structure is shown in Figure 3. The circular macrocycle of  $\beta$ CD is deformed to an ellipse with complex formation. This structure is qualitatively consistent with the observed NMR data mentioned above [15].

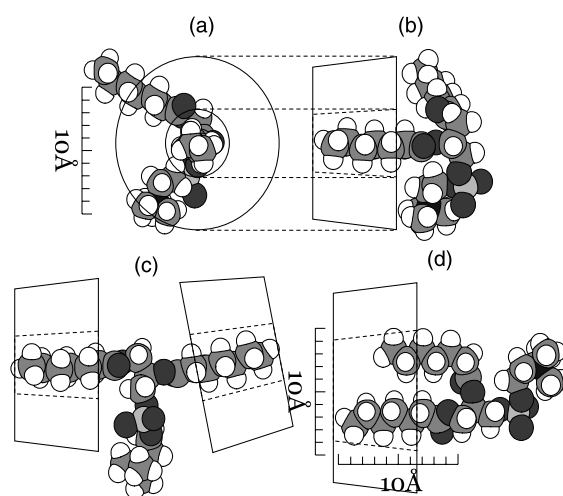


Figure 2. Structures of three major complexes of DHPC with  $\alpha$ CD and  $\gamma$ CD: (a) side view of *G*<sup>-</sup> $\alpha$ CD, (b) top view of *G*<sup>-</sup> $\alpha$ CD, (c) *T*( $\alpha$ CD)<sub>2</sub>, and (d) *G*<sup>+</sup> $\gamma$ CD [14].

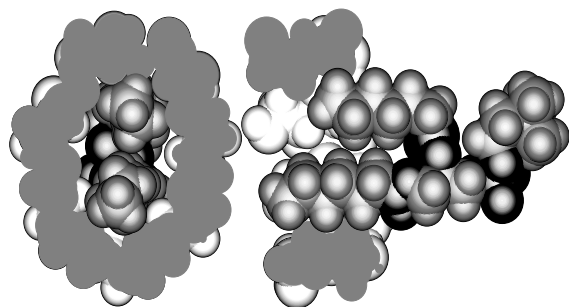


Figure 3. Top and side views of energetically optimized structure of the  $G^+-\beta$ CD complex [15].

One of the serious toxicities of CDs is hemolysis. This hemolysis results from the extraction of phospholipid and cholesterol from human erythrocyte membranes. The hemolytic activity is strong in the order  $\beta$ CD  $>$   $\alpha$ CD  $>$   $\gamma$ CD [24]. The 1:1 binding constant of DHPC is large in the order  $\beta$ CD  $>$   $\gamma$ CD  $>$   $\alpha$ CD, though the 1:2 binding constant of  $\alpha$ CD is much larger than that of  $\gamma$ CD [15]. Thus, the binding capacity of the CDs to DHPC is consistent with the hemolytic activity. Phospholipid in the erythrocyte membrane has long acyl chains. The ratios of long-chain phospholipid to  $\alpha$  or  $\gamma$ CD are explicable on the basis of the structures of the DHPC complexes with  $\alpha$ CD and  $\gamma$ CD [14].

### Dialkyldimethylammonium bromide-CD system

Dialkyldimethylammonium bromide is a simpler double-chain compound than lecithin. Complex formation between didecyltrimethylammonium bromide (DDAB) and CDs was investigated with a DDAB-selective electrode. This electrode normally responded the DDAB concentration between 0.00036 and 0.5 mM. The effect of  $\alpha$ CD on the electromotive force of a 0.5 mM DDAB solution is shown in Figure 4. As the  $\alpha$ CD concentration was increased, the electromotive force decreased. This decrease results from the decrease in free DDAB concentration. The 1:1 + 1:2 complex model (dashed line in Figure 4) was best fitted to the observed electromotive forces and the macroscopic 1:1 and 1:2 binding constants were obtained (Table 1). The 1:1 model (solid line) is worse than this model. In a similar way, the macroscopic 1:1 and 1:2 binding constants were obtained for  $\beta$ CD and  $\gamma$ CD (Table 1). Although  $\gamma$ CD forms the 1:1 complex alone,  $\alpha$ CD and  $\beta$ CD form the 1:1 and 1:2 complexes. Thus, although DDAB is a univalent substrate to  $\gamma$ CD, it is a bivalent substrate to  $\alpha$ CD and  $\beta$ CD. Two decyl chains of DDAB will be incorporated in a  $\gamma$ CD cavity simultaneously. Because these chains of DDAB are tightly bound to the  $\gamma$ CD cavity, the 1:1 binding constant is larger than that for dodecyltrimethylammonium bromide and  $\gamma$ CD (Table 1) [16].

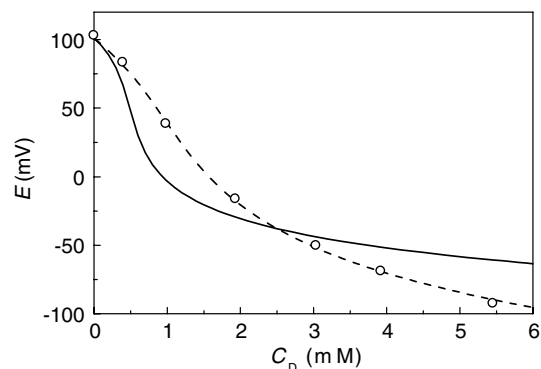


Figure 4. Effect of  $\alpha$ CD on the electromotive force of 0.5 mM DDAB. The solid and dashed lines show the 1:1 and 1:1 + 1:2 models, respectively [16].

Table 1. Binding constants of DDAB and related surfactants with CDs [16]

CD	1:1 model	1:1 + 1:2 model	
	$K_1$ ( $M^{-1}$ )	$K_1$ ( $M^{-1}$ )	$K_2$ ( $M^{-1}$ )
<i>DDAB</i>			
$\alpha$ CD	120,000	15,900	5700
$\beta$ CD	51,000	16,100	730
$\gamma$ CD	4310	4440	$1.8 \times 10^6$
<i>Dodecyltrimethylammonium bromide</i>			
$\alpha$ CD	17,000	17,000	1000
$\beta$ CD	17,000		
$\gamma$ CD	110		
<i>Sodium decyl sulfate</i>			
$\beta$ CD		8750	58

DDAB has two equivalent binding sites. If these sites independently bind to CD, we can expect that Equations (9) and (10) are applicable. When the macroscopic 1:1 binding constant for sodium decyl sulfate and  $\beta$ CD was used as the microscopic 1:1 binding constant (Table 1), the theoretical  $K_1$  and  $K_2$  values for DDAB are 17,500 and 4400  $M^{-1}$ . These theoretical values are very close to the observed ones for  $\alpha$ CD. Therefore, two decyl chains of DDAB independently bind to  $\alpha$ CD. They also independently bind to  $\beta$ CD to form the 1:1 complex, but the second binding of the decyl chain is inhibited slightly [16].

The octyl chain of hexyldimethyloctylammonium bromide (HDOAB) is distinguishable from the hexyl chain in the proton NMR spectrum. The  $\omega$ -methyl protons ( $H_{\omega 8}$  and  $H_{\omega 6}$ ) of HDOAB have the same chemical shift as those of octyltrimethylammonium (OTAB) and hexyltrimethylammonium (HTAB) bromides, respectively [23]. From the concentration dependence of chemical shifts, we determined the  $K_1$  (1890  $M^{-1}$ ),  $K_2$  (300  $M^{-1}$ ),  $\Delta\delta_{SD}$ , and  $\Delta\delta_{SD_2}$  values (Figure 5). The observed  $\Delta\delta_{SD}$  values for  $\alpha$ CD complexes with OTAB and HTAB are 0.036 and 0.117 ppm,

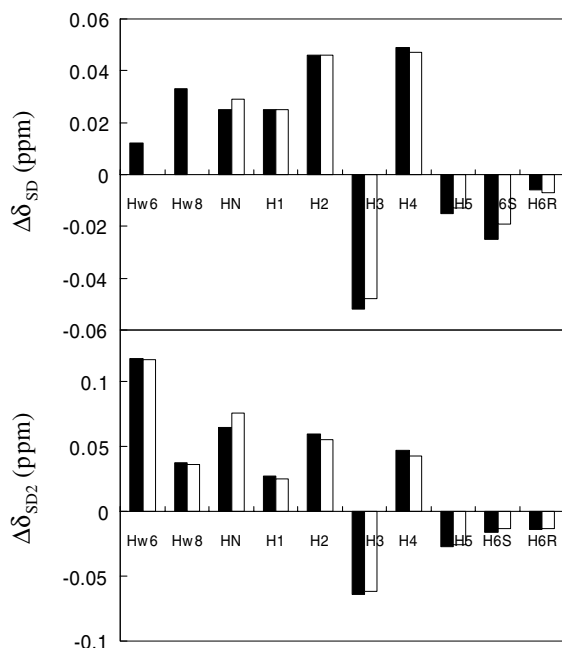


Figure 5. The observed (open squares) and theoretical (closed squares)  $\Delta\delta_{SD}$  and  $\Delta\delta_{SD_2}$  values for the 1:1 and 1:2 complexations between HDOAB and  $\alpha$ CD (N. Funasaki *et al.*, submitted for publication).

respectively [23]. These are very close to the  $\Delta\delta_{SD_2}$  (H $\omega$ 8 and H $\omega$ 6) values of HDOAB values. This finding indicates that the octyl and hexyl chains independently bind to  $\alpha$ CD and that the magnetic environments around the  $\omega$ -methyl groups (H $\omega$ 8 and H $\omega$ 6) in the 1:2 complex are close to those in the 1:1 complexes with OTAB and HTAB, respectively (N. Funasaki *et al.*, submitted for publication).

The  $\Delta\delta_{SD}$ (H $\omega$ 8) and  $\Delta\delta_{SD}$ (H $\omega$ 6) values for HDOAB are 0.033 and 0.012 ppm, which are smaller than those for OTAB and HTAB [23]. These differences are ascribed to partial binding of the  $\omega$ -methyl groups in the 1:1 complex of HDOAB. For the octyl-in complex (XDY) the  $\omega$ -methyl proton of the hexyl group of HDOAB will not be influenced magnetically, whereas the  $\omega$ -methyl proton of the octyl group is fully bound to  $\alpha$ CD. Therefore, we can expect that  $\Delta\delta_{XDY}$ (H $\omega$ 8) is set to be equal to  $\Delta\delta_{SD}$ (H $\omega$ 8, OTAB) and  $\Delta\delta_{XDY}$ (H $\omega$ 6) is zero. Substituting these values into Equation (13), we can estimate the mole fraction  $x_8$  of the octyl-in complex in the 1:1 complex from

$$\begin{aligned} x_8 &= \Delta\delta_{SD}(\text{HDOAB})/\Delta\delta_{SD}(\text{OTAB}) \\ &= 0.033/0.036 = 0.916 \end{aligned} \quad (14)$$

In a similar way, we can estimate the mole fraction  $x_6$  of the hexyl-in complex in the 1:1 complex from

$$\begin{aligned} x_6 &= \Delta\delta_{SD}(\text{HDOAB})/\Delta\delta_{SD}(\text{HTAB}) \\ &= 0.012/0.117 = 0.102 \end{aligned} \quad (15)$$

The sum of these mole fractions is 1.018, which is very close to 1.000. Furthermore, substituting these mole fractions,  $\Delta\delta_{XDY}(\text{HDOAB}) = \Delta\delta_{XDY}(\text{OTAB})$ , and  $\Delta\delta_{XDY}(\text{HDOAB}) = \Delta\delta_{XDY}(\text{HTAB})$ , we can calculate the theoretical  $\Delta\delta_{SD}$  values for HDOAB and  $\alpha$ CD protons from Equation (13). For the 1:2 complex, the theoretical  $\Delta\delta_{SD_2}(\text{HDOAB})$  values for the  $\alpha$ CD protons can be calculated from

$$\begin{aligned} \Delta\delta_{SD_2}(\text{HDOAB}) \\ &= [\Delta\delta_{SD}(\text{OTAB}) + \Delta\delta_{SD}(\text{HTAB})]/2 \end{aligned} \quad (16)$$

As shown in Figure 5, these theoretical  $\Delta\delta_{SD}(\text{HDOAB})$  and  $\Delta\delta_{SD_2}(\text{HDOAB})$  values are in an excellent agreement with the observed ones.

This agreement allows us to estimate the structures of the 1:1 and 1:2 complexes: the octyl and hexyl groups of HDOAB in the 1:1 and 1:2 complexes has the same geometry as those in the 1:1 complexes between OTAB and  $\alpha$ CD as well as HTAB and  $\alpha$ CD [23]. Thus, the structures of the 1:1 and 1:2 complexes estimated are shown in Figure 6 (N. Funasaki *et al.*, submitted for publication).

Thus, the octyl and hexyl groups independently bind to  $\alpha$ CD. This conclusion is also supported by the binding constant data on HDOAB, HTAB, and OTAB (N. Funasaki *et al.*, submitted for publication).

## OB-CD system

Oxyphenonium bromide (OB, Figure 7) has the phenyl and cyclohexyl groups that can bind to CDs. The UV absorbance and electromotive force data established that OB forms the 1:1 complexes with  $\alpha$ CD,  $\beta$ CD, and  $\gamma$ CD, although it does not form any 1:2 complex [25, 26].

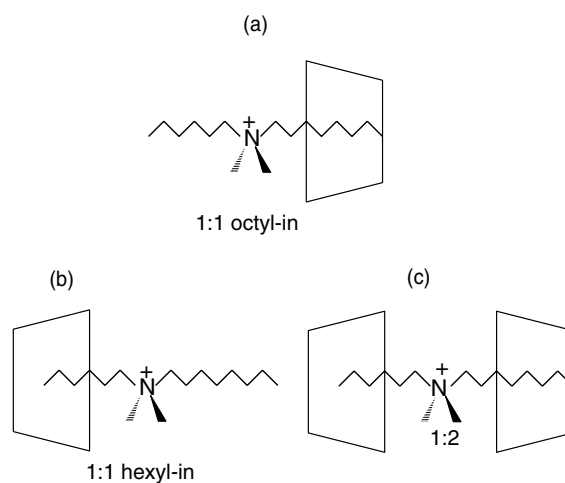


Figure 6. Structures of (a) the octyl-in, (b) the hexyl-in, and (c) the 1:2 complexes of HDOAB and  $\alpha$ CD (N. Funasaki *et al.*, submitted for publication).

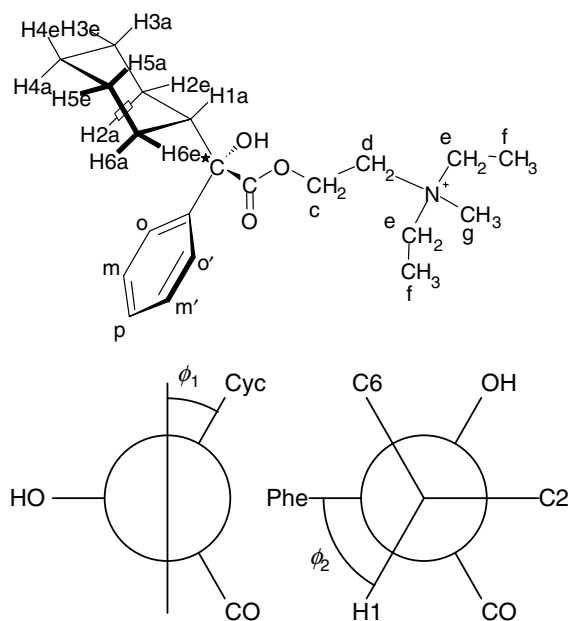


Figure 7. Chemical structure of oxyphenium bromide (OB) and the Newman projection [22].

A detailed structure of the 1:1 complex of OB with  $\alpha$ CD was estimated from the ROESY spectrum, chemical shifts, molecular mechanics calculations, and molecular surface area calculations. In the ROESY spectrum of aqueous solution containing 40 mM OB and 40 mM  $\alpha$ CD, both of the phenyl and cyclohexyl protons of OB exhibited intermolecular cross-peaks with  $\alpha$ CD protons. This result indicates that both of the phenyl and cyclohexyl groups are incorporated in the  $\alpha$ CD cavity to form two kinds of 1:1 complexes, the cyclohexyl-in complex and the phenyl-in complex. The volume (ROE intensity) of the cross-peak was determined by integration. The ROE intensity of the cross peak is proportional to the number of equivalent protons. When internal rotations of a molecule are slower than the overall tumbling, we can expect the following relation [22]:

$$\text{ROE} = k \sum_{i=1}^{n_{\text{CD}}} \sum_{j=1}^{n_{\text{OB}}} d_{\text{CD}i\text{OB}j}^{-6} \quad (17)$$

Here,  $d_{\text{CD}i\text{OB}j}$  denotes the distance between a proton (CD*i*) of CD and a proton (OB*j*) of OB, and  $n_{\text{CD}}$  and  $n_{\text{OB}}$  stand for the number of equivalent protons of the  $\alpha$ CD and OB group, respectively. For simplicity, the effective distance ( $d_{\text{eff}}$ ) is defined as

$$(d_{\text{eff}})^{-6} = (1/n_{\text{CD}}n_{\text{OB}}) \sum_{i=1}^{n_{\text{CD}}} \sum_{j=1}^{n_{\text{OB}}} d_{\text{CD}i\text{OB}j}^{-6} \quad (18)$$

From Equations (17) and (18) we can expect that  $\text{ROE}/n_{\text{CD}}n_{\text{OB}}$  increases as two protons become closer to each other.

Based on these NOE data, we imagined rough structures of the phenyl-in and cyclohexyl-in complexes.

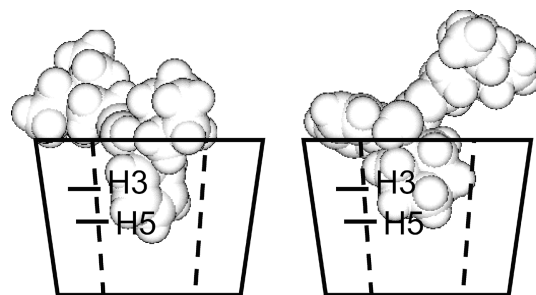


Figure 8. Three-dimensional structures of the phenyl-in and cyclohexyl-in complex of OB and  $\alpha$ CD estimated by molecular mechanics and NMR [22].

Furthermore, these structures were energy-minimized by molecular mechanics calculations, as shown in Figure 8. On the basis of these molecular mechanics structures, we calculated the effective distance ( $d_{\text{eff}}$ ) and plotted it against the ROE intensity ( $\text{ROE}/n_{\text{CD}}n_{\text{OB}}$ ). As expected from Equations (17) and (18),  $\text{ROE}/n_{\text{CD}}n_{\text{OB}}$  decreases with increasing  $d_{\text{eff}}$  (Figure 9). This finding indicates that the structures of the phenyl-in and cyclohexyl-in complexes are reasonable [22].

The mole fractions of the phenyl-in and cyclohexyl-in complexes were estimated from the chemical shift variations and binding constants of related substrates. If the observed chemical shift variations of the phenyl protons result from the phenyl-in complexation, they should be equal to those at full binding multiplied by the mole fraction of the phenyl-in complex. The chemical shift variations of the phenyl protons at full binding were estimated from those for the benzenesulfonate- $\alpha$ CD complex [21]. Thus, the mole fraction of the phenyl-in complex was estimated to be 0.4. Another estimation comes from the binding constants of phenol ( $19.8 \text{ M}^{-1}$ ) and cyclohexanol ( $56 \text{ M}^{-1}$ ) with  $\alpha$ CD. If we employ these values for the phenyl-in and cyclohexyl-in complexations in Equation (7), we can estimate a binding constant of  $75.8 \text{ M}^{-1}$  for OB. This is very close

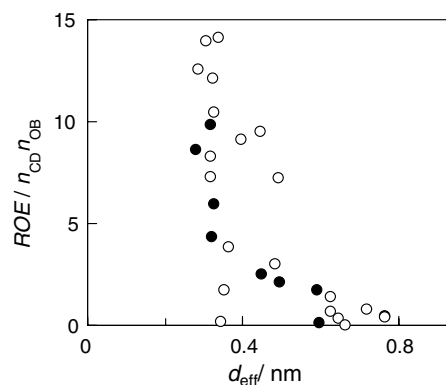


Figure 9. Observed  $\text{ROE}/n_{\text{CD}}n_{\text{OB}}$  values plotted against the effective proton-proton distances calculated for the phenyl protons (closed circles) of the phenyl-in complex and the cyclohexyl protons (open circles) of the cyclohexyl-in complex in the structures shown in Figure 8 [22].

to our NMR value ( $70 \text{ M}^{-1}$ ). This agreement also supports the coexistence of two kinds of complexes of OB and  $\alpha\text{CD}$ , and allows us to estimate the mole fractions of these complexes; the mole fractions of the phenyl-in and cyclohexyl-in complexes are 0.3 and 0.7, respectively. The third estimation is based on molecular surface areas. Molecular surface area calculations predicted the structures of the phenyl-in and cyclohexyl-in complexes close to the molecular mechanics structure (Figure 8). From these structures, we estimated the binding constants and mole fractions of the phenyl-in and cyclohexyl-in complexes [22].

The conformational change of OB with  $\alpha\text{CD}$  complexation was estimated from the chemical shift variation of the cyclohexyl protons. The chemical shifts of the cyclohexyl protons are very sensitive to the configuration of the phenyl group, namely, to the dihedral angles ( $\varphi_1$  and  $\varphi_2$ ) as defined in Figure 7. OB has four pairs of corresponding protons (H2a and H6a, H2e and H6e, H3a and H5a, and H3e and H5e). The chemical shifts of the paired protons are different from each other. This magnetic nonequivalence was ascribed to the difference in the ring-current effects of the phenyl group on the paired protons [22]. The observed chemical-shift differences for four pairs of the protons were best fitted to those calculated based on the ring-current effect by regarding the dihedral angles as being adjustable parameters to determine the structure of OB in the free state [22]. This NMR structure is shown by the light lines of Figure 10. This procedure was employed to estimate the average structure of OB in the OB- $\alpha\text{CD}$  complex; we could not separately determine the structures of OB in the phenyl-in complex and in the cyclohexyl-in complex. This structure of the complex, shown by the dark lines of Figure 10, is less crowded than that of the free OB molecule (light lines). This induced structural change will facilitate the complexation of OB with  $\alpha\text{CD}$  [22].

OB is a bitter anticholinergic drug. This bitter taste can be reduced by CDs, because these complexes do not taste bitter [25, 26]. Generally, bitter compounds are

hydrophobic. For instance, OB has the hydrophobic phenyl and cyclohexyl groups. However, these groups are incorporated in CD cavities (see Figure 8 for the OB- $\alpha\text{CD}$  complexes). The phenyl and cyclohexyl groups are also accommodated in  $\beta\text{CD}$  and  $\gamma\text{CD}$  cavities (unpublished data). Therefore, these complexes do not taste bitter. The bitter intensity was determined by the concentration of OB in the free state, regardless of the amount and kinds of the OB-CD complexes. The concentration of OB in the free state was determined from the electromotive force of an OB-selective electrode [26]. Thus, the bitter taste intensity of all aqueous solutions containing OB and CDs can be determined from the electromotive force without human sensory tests [26].

The dielectric constant around the microenvironment of OB in a complexed state may be estimated from the UV maximum wavelength [25]. A detailed structure of the OB-CD complex provides a basis for this estimation of the dielectric constant. The ester group of OB is hydrolyzed in alkaline solutions. The hydrolysis is slightly accelerated by  $\alpha\text{CD}$ , whereas it is remarkably decelerated by  $\beta\text{CD}$  and  $\gamma\text{CD}$ . These changes in hydrolysis rate are explained on the basis of the structures of the OB complexes with  $\alpha\text{CD}$ ,  $\beta\text{CD}$ , and  $\gamma\text{CD}$  [27].

## Conclusions

The interactions between cyclodextrin and substrates having two binding sites in aqueous solution are reviewed. For such substrates, multiple equilibria, NMR chemical shift variations with full binding, solution structures of complexes, and the effects of cavity size are analyzed quantitatively. The solution structures of complexes play a crucial role in these basic researches as well as the applications of cyclodextrin, such as bitter taste reduction and stabilization of labile substrates. Many other multiple substrates are known [8–11]. For instance, 1,4-di-substituted benzenes are rather well investigated [8]. Single long-chain surfactants having 10 or more carbon atoms can bind two CD molecules. Dimeric cyclodextrins, in which two CD molecules are bound chemically, can be also treated in the same way as bivalent substrates. The present approach to CD complexes will be also useful in supramolecular chemistry [28, 29].

## Acknowledgements

Thanks are due to Dr. Seiji Ishikawa for his excellent drawing of figures. The work was supported by a Grant-in-Aid for the Frontier Research Program of the Ministry of Education, Science, Sports, and Culture of Japan.

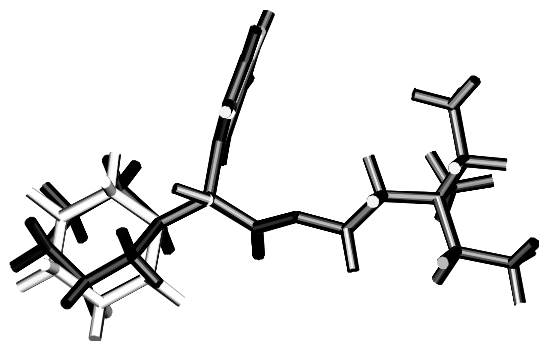


Figure 10. Three-dimensional structures of OB in the free state (light lines) and in the complexed (dark lines) estimated from chemical shifts of cyclohexyl protons [22].

## References

1. M.L. Bender and M. Komiyama: *Cyclodextrin Chemistry*, Chap. 2 and 3, Springer-Verlag, Berlin (1978).
2. J. Szejtli and T. Osa (eds.): *Cyclodextrins*, Pergamon, London (1996).
3. H.-J. Schneider, F. Hacket, V. Rüdiger, and H. Ikeda: *Chem. Rev.* **98**, 1755 (1998).
4. W. Saenger, J. Jacob, K. Gesseler, T. Steiner, D. Hoffmann, H. Sanbe, K. Koizumi, S. Smith, and T. Takaha: *Chem. Rev.* **98**, 1787 (1998).
5. K. Harata: *Chem. Rev.* **98**, 1803 (1998).
6. K.B. Lipkowitz: *Chem. Rev.* **98**, 1829 (1998).
7. M.V. Rekharsky and Y. Inoue: *Chem. Rev.* **98**, 1875 (1998).
8. K.A. Connors: *Chem. Rev.* **97**, 1325 (1997).
9. A. Harada: *Acc. Chem. Res.* **34**, 456 (2001).
10. N. Funasaki: *Karhkov Univ. Bull.* No. **549**, 1 (2002).
11. K.A. Connors: *Binding Constants*, Chap. 2, John Wiley and Sons, New York (1987).
12. C. Tanford: *Physical Chemistry of Macromolecules*, Chap. 8, John Wiley and Sons, New York (1961).
13. N. Funasaki, H. Yodo, S. Hada, and S. Neya: *Bull. Chem. Soc. Jpn.* **65**, 1323 (1992).
14. S. Ishikawa, S. Neya, and N. Funasaki: *J. Phys. Chem. B* **102**, 2502 (1998).
15. N. Funasaki, S. Ishikawa and S. Neya: *Langmuir* **18**, 1786 (2002).
16. N. Funasaki and S. Neya: *Langmuir* **16**, 5343 (2000).
17. Y. Matsui and S. Tokunaga: *Bull. Chem. Soc. Jpn.* **69**, 2477 (1996).
18. N. Funasaki, M. Nomura, H. Yamaguchi, S. Ishikawa, and S. Neya: *Bull. Chem. Soc. Jpn.* **73**, 2727 (2000).
19. N. Funasaki, M. Nomura, S. Ishikawa, and S. Neya: *J. Phys. Chem. B* **105**, 7361 (2001).
20. N. Funasaki, H.S. Ishikawa, and S. Neya: *Bull. Chem. Soc. Jpn.* **75**, 719 (2002).
21. N. Funasaki, H. Yamaguchi, S. Ishikawa, and S. Neya: *J. Phys. Chem. B* **105**, 760 (2001).
22. N. Funasaki, H. Yamaguchi, S. Ishikawa, and S. Neya: *Bull. Chem. Soc. Jpn.* **76**, 903 (2003), and references therein.
23. N. Funasaki, S. Ishikawa, and S. Neya: *J. Phys. Chem. B* **107**, 10094 (2003).
24. N. Funasaki, M. Ohigashi, S. Hada, and S. Neya: *Langmuir* **2000**, **16**, 383, and references therein.
25. N. Funasaki, K. Kawaguchi, S. Hada, and S. Neya: *J. Pharm. Sci.* **88**, 759 (1999).
26. N. Funasaki, K. Kawaguchi, S. Ishikawa, S. Hada, S. Neya, and T. Katsu: *Anal. Chem.* **71**, 1733 (1999).
27. N. Funasaki, S. Ishikawa, and S. Neya: *J. Pharm. Sci.* **90**, 740 (2001).
28. M.-J. Lehn: *Supramolecular Chemistry*, VCH Verlag, Berlin (1995).
29. H.-J. Schneider and A. Yatsimirsky: *Principles and Methods in Supramolecular Chemistry*, Wiley, New York (2000).